

## Anomalous Suppression of the Orthorhombic Lattice Distortion in Superconducting Ba(Fe<sub>1-x</sub>Co<sub>x</sub>)<sub>2</sub>As<sub>2</sub> Single Crystals

S. Nandi, M. G. Kim, A. Kreyssig, R. M. Fernandes, D. K. Pratt, A. Thaler, N. Ni, S. L. Bud'ko, P. C. Canfield, J. Schmalian, R. J. McQueeney, and A. I. Goldman\*

Ames Laboratory, U.S. DOE and Department of Physics and Astronomy, Iowa State University, Ames, Iowa 50011, USA  
(Received 11 November 2009; published 5 February 2010)

High-resolution x-ray diffraction measurements reveal an unusually strong response of the lattice to superconductivity in Ba(Fe<sub>1-x</sub>Co<sub>x</sub>)<sub>2</sub>As<sub>2</sub>. The orthorhombic distortion of the lattice is suppressed and, for Co doping near  $x = 0.063$ , the orthorhombic structure evolves smoothly back to a tetragonal structure. We propose that the coupling between orthorhombicity and superconductivity is indirect and arises due to the magnetoelastic coupling, in the form of emergent nematic order, and the strong competition between magnetism and superconductivity.

DOI: 10.1103/PhysRevLett.104.057006

PACS numbers: 74.70.Xa, 61.50.Ks, 74.62.Bf, 74.70.Ad

The interplay between superconductivity, magnetism, and structure has become a major theme of research in the iron arsenide families [1,2] of superconductors. The strong coupling between magnetism and structure, for example, is illustrated by the parent compounds, AEF<sub>2</sub>As<sub>2</sub> (AE = Ba, Sr, Ca), which manifest simultaneous transitions from a paramagnetic, tetragonal phase to an antiferromagnetically ordered, orthorhombic phase [3–5]. Strong coupling is also evidenced by recent inelastic x-ray [6] and neutron [7] scattering measurements of lattice excitations, and Raman spectroscopy [8]; all require consideration of magnetic ordering or fluctuations to obtain reasonable agreement with theory. Strong coupling between superconductivity and magnetism are observed in several inelastic neutron scattering measurements [9–15], which highlight the appearance of a resonance, or opening of a spin gap, in the magnetic fluctuation spectrum below the superconducting transition ( $T_c$ ) in doped AEF<sub>2</sub>As<sub>2</sub> and LaFeAsO compounds. Perhaps most striking is the observation that the static magnetic order for Co-doped BaFe<sub>2</sub>As<sub>2</sub> is significantly suppressed below  $T_c$  [14,15].

Here we describe high-resolution x-ray diffraction measurements that demonstrate an unusually strong response of the lattice to superconductivity in Ba(Fe<sub>1-x</sub>Co<sub>x</sub>)<sub>2</sub>As<sub>2</sub>. Below  $T_c$ , the orthorhombic distortion of the lattice is significantly suppressed and, for  $x \approx 0.063$ , the orthorhombic structure evolves smoothly back to a tetragonal structure. Our observations are consistent with a strong magnetoelastic coupling, realized through emergent nematic order that manifests orientational order in the absence of long-range positional order, analogous to the nematic phase in liquid crystals. For the iron arsenide compounds, the nematic phase corresponds to orientational order between two antiferromagnetic sublattices, with staggered magnetizations,  $\mathbf{m}_1$  and  $\mathbf{m}_2$ , that are only weakly coupled because of frustration that arises from large next-nearest-neighbor magnetic interactions [16–18]. The ne-

matic order parameter is defined as  $\varphi = \mathbf{m}_1 \cdot \mathbf{m}_2$ . Above the structural transition at  $T_S$ , the time-averaged quantities,  $\langle \varphi \rangle = 0$  and  $\langle \mathbf{m}_1 \rangle = \langle \mathbf{m}_2 \rangle = 0$ . With the onset of nematic ordering at  $T_S$ ,  $\langle \varphi \rangle \neq 0$ , while  $\langle \mathbf{m}_1 \rangle = \langle \mathbf{m}_2 \rangle = 0$ , resulting in nematic order, but no static magnetic order. Below  $T_N$ ,  $\langle \varphi \rangle \neq 0$  and static magnetic order sets in with  $\langle \mathbf{m}_1 \rangle \neq 0$  and  $\langle \mathbf{m}_2 \rangle \neq 0$ . The nematic degree of freedom leads to the structural distortion which lifts the magnetic frustration [19–21]. Within this picture, the competition between the orthorhombic distortion and superconductivity is rooted in the coupling between magnetism and superconductivity [14,15]; i.e., there is a common origin for the suppression of both the structural and magnetic order parameters below  $T_c$ .

Single crystals of Ba(Fe<sub>1-x</sub>Co<sub>x</sub>)<sub>2</sub>As<sub>2</sub> were grown out of a FeAs self-flux using conventional high temperature solution growth [22]. Details of the growth procedures are provided in Ref. [22]. The compositions were measured at between 10 and 30 positions on samples from each growth batch using wavelength dispersive spectroscopy (WDS). The combined statistical and systematic error on the Co composition is not greater than 5% (e.g.,  $0.063 \pm 0.003$ ). Since we have studied a set of samples with Co concentrations within the error stated above, it is important to establish that there are, indeed, systematic variations in sample properties across our compositional range. To this end, in Fig. 1(a), we plot both the tetragonal-to-orthorhombic transition temperature  $T_S$ , determined from our x-ray measurements, and  $T_c$ , as determined from the onset of the superconducting transition in the magnetization data in Fig. 1(b). These data clearly establish that both  $T_c$  and  $T_S$  change systematically with the average Co composition determined by WDS, and we will employ these values in the remainder of this Letter. We further note that the structural, compositional, thermodynamic, and transport measurements on samples from each batch are consistent with the data presented in Ref. [22]. Figure 1(b) shows that all samples exhibit relatively sharp

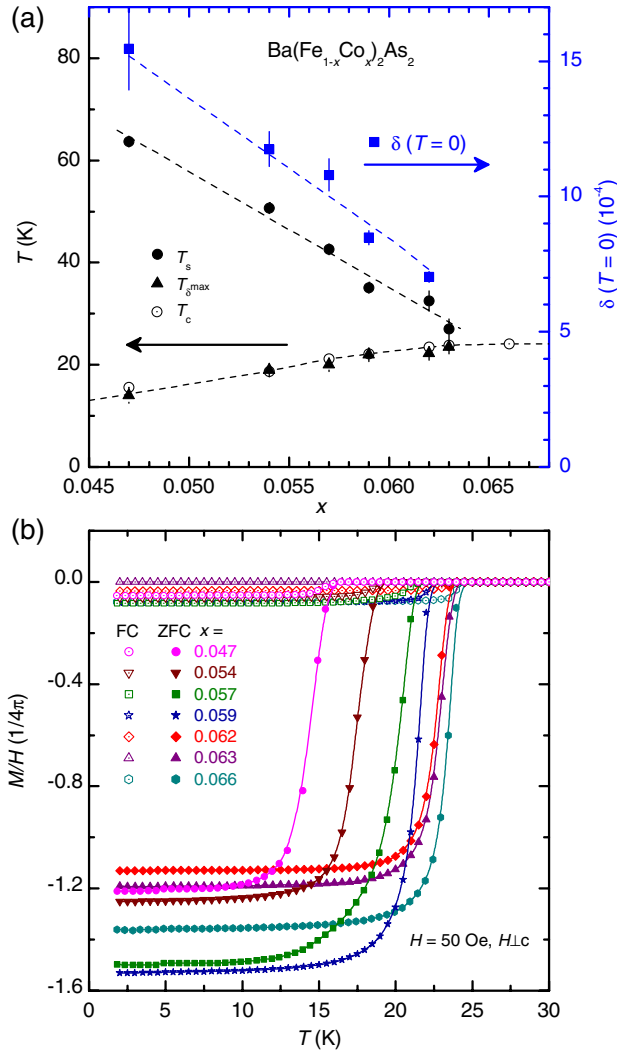


FIG. 1 (color online). (a) Tetragonal-to-orthorhombic transition temperature  $T_S$  (filled circles) and superconducting transition temperature  $T_c$  (open circles) from the present measurements as a function of the average value of Co doping as determined from WDS. The filled triangles and squares represent  $T_\delta^{\max}$  and  $\delta(0)$  as described in the text. Dashed lines serve as guides to the eye. (b) The zero-field cooled and field cooled magnetization for all samples in this study.

superconducting transitions and we find no anomalies or measurable changes in the magnetization at temperatures below  $T_c$ , indicating that the superconducting volume fraction does not evolve below  $T_c$ .

Temperature-dependent, high-resolution, single-crystal x-ray diffraction measurements were performed on a four-circle diffractometer using Cu  $K_{\alpha 1}$  radiation from a rotating anode x-ray source, selected by a germanium (1 1 1) monochromator. For these measurements, the plate-like single crystals with typical dimensions of  $3 \times 3 \times 0.5$  mm<sup>3</sup> were attached to a flat copper sample holder on the cold finger of a closed-cycle displax refrigerator. The mosaicities of the Ba(Fe<sub>1-x</sub>Co<sub>x</sub>)<sub>2</sub>As<sub>2</sub> single crystals were all less than 0.02° full-width-at-half-maximum as mea-

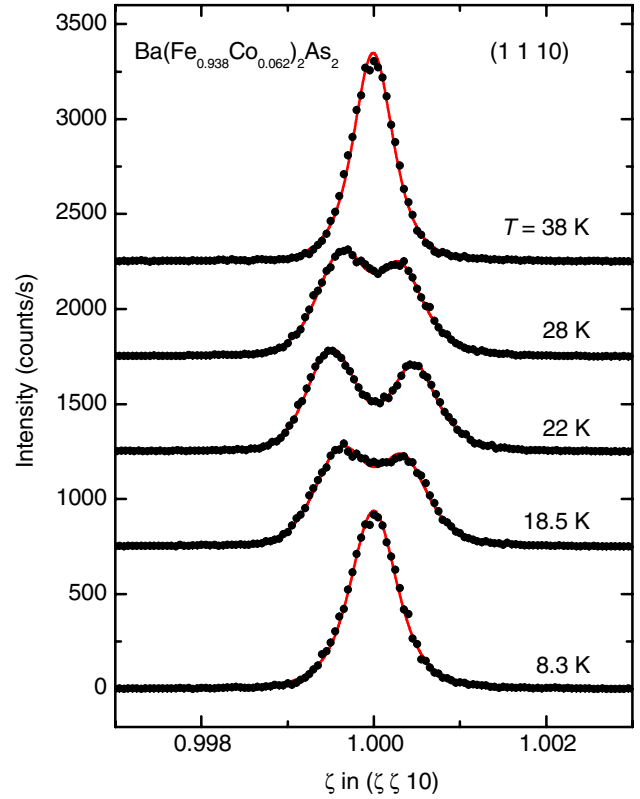


FIG. 2 (color online). Temperature evolution of the (1 1 10) Bragg peak in Ba(Fe<sub>0.938</sub>Co<sub>0.062</sub>)<sub>2</sub>As<sub>2</sub> at several temperatures. The red lines represent fits to the data using either one (for  $T = 38$  K and 8.3 K) or two (for  $T = 28$  K, 22 K and 18.5 K) Lorentzian squared peaks. For this sample,  $T_S = 32$  K and  $T_c = 23$  K.

sured by the rocking curve of the (1 1 10) reflection at room temperature. The diffraction data were obtained as a function of temperature between room temperature and 8 K, the base temperature of the refrigerator.

Figure 2 shows a subset of ( $\zeta \zeta 0$ ) scans through the (1 1 10) reflection for Ba(Fe<sub>0.938</sub>Co<sub>0.062</sub>)<sub>2</sub>As<sub>2</sub> as the sample was cooled through  $T_S = 32 \pm 1$  K. The splitting of the peak below  $T_S$  is consistent with the structural transition, from space group  $I4/mmm$  to  $Fmmm$ , with a distortion along the [1 1 0] direction. As the sample is cooled further, the orthorhombic splitting increases until  $T_c = 23 \pm 1$  K. Lowering the temperature below  $T_c$  results in a smooth decrease in the orthorhombic distortion until, below approximately 13 K, a single component line shape reproduces the data.

In order to map systematic changes in structure with composition, the temperature dependence of the orthorhombic distortion,  $\delta = \frac{(a-b)}{(a+b)}$ , was measured for a series of seven Ba(Fe<sub>1-x</sub>Co<sub>x</sub>)<sub>2</sub>As<sub>2</sub> samples, with  $0.047 \leq x \leq 0.066$ , and is displayed in Fig. 3. The solid symbols in Fig. 3 represent  $\delta$ , as determined from fits to the ( $\zeta \zeta 0$ ) scans using two Lorentzian squared peaks. For the  $x = 0.062$  and  $x = 0.063$  samples at low temperature, however,

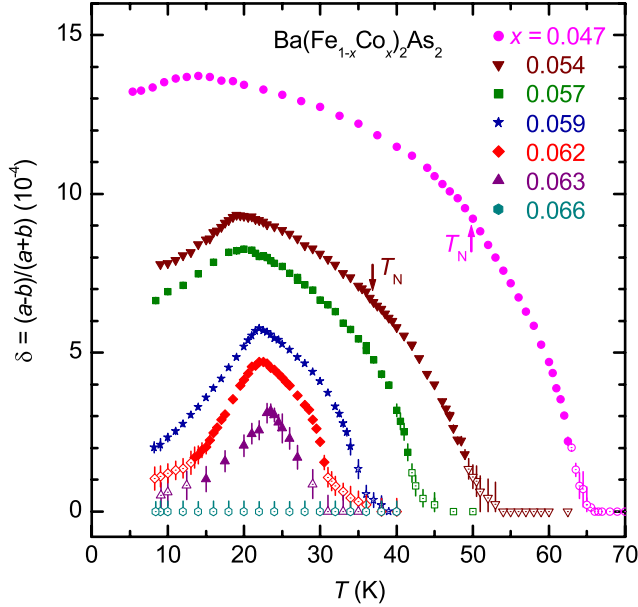


FIG. 3 (color online). The measured orthorhombic distortion  $\delta$  as a function of temperature. Filled symbols represent the distortion determined from the positions of two peak fits to the data. The open symbols represent an upper limit on the distortion extracted from the line broadening of a single peak fit to the data relative to the peak width well above  $T_S$ . Labeled arrows denote the measured  $T_N$  for several samples.

a single peak was sufficient, as demonstrated in Fig. 2. The open symbols in Fig. 3 represent an upper limit on  $\delta$  based on the residual broadening of a single peak fit to the data, with respect to the peak width determined from scans well above  $T_S$ .

The relative decrease in the orthorhombicity below  $T_c$  is pronounced and increases with increased doping. Indeed, the  $x = 0.063$  sample exhibits reentrant behavior, within experimental uncertainty, where the low-temperature structure returns to tetragonal symmetry below  $T_c$ . For  $x = 0.066$ , no transition to the orthorhombic structure was observed, defining an upper Co concentration limit for the tetragonal-to-orthorhombic phase transition. To place the magnitude of the suppression of the orthorhombicity in some context, we note that ultrahigh-resolution thermal expansion measurements on untwinned single crystals of  $\text{YBa}_2\text{Cu}_3\text{O}_{7-\delta}$  also found a change in the orthorhombic distortion at  $T_c$ , but smaller than the present case by approximately 2 orders of magnitude [23].

With these results in hand, we have refined the phase diagram, shown in Fig. 4, to indicate how the phase line representing the tetragonal-to-orthorhombic transition bends back below  $T_c$ . We also plot, in Fig. 1(a), both the temperature,  $T_\delta^{\text{max}}$ , at which the orthorhombic distortion for a given sample is at a maximum, and  $\delta(0)$ , the  $T = 0$  extrapolated value for  $\delta$  determined from a power law fit to the data above  $T_c$ . We find that  $T_\delta^{\text{max}}$  is coincident with  $T_c$  for all samples, and the monotonic decrease in  $\delta(0)$  with increasing Co doping is consistent with the decrease in  $T_S$

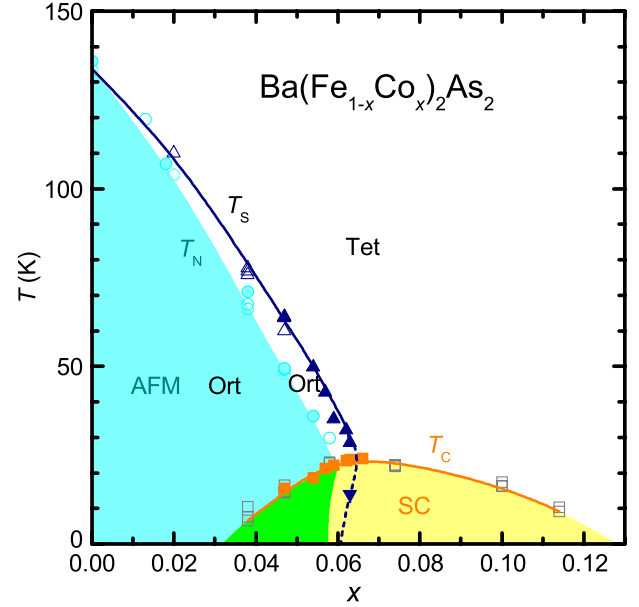


FIG. 4 (color online). The  $T$ - $x$  phase diagram for  $\text{Ba}(\text{Fe}_{1-x}\text{Co}_x)_2\text{As}_2$  compiled from data in Refs. [22] (open symbols), [24] (filled symbols for  $T_N$ ), and the present study (filled symbols for  $T_S$  and  $T_c$ ). The extension of the tetragonal-to-orthorhombic phase line into the superconducting dome is represented by the dashed line.

for each sample. Furthermore, an extrapolation of the dashed line to  $x = 0$  finds agreement with the value of  $\delta(0)$  for the parent  $\text{BaFe}_2\text{As}_2$  compound.

The strong suppression of the structural order parameter at low temperatures is highly unusual and clearly connected to the onset of superconductivity. The leading coupling in a Landau expansion of the free energy between the orthorhombic distortion  $\delta$  and the superconducting order parameter  $|\Psi|$  is  $\frac{\gamma_\delta}{2} \delta^2 |\Psi|^2$ . In principle, one could rationalize our results as arising from a strong competition between orthorhombic order and superconductivity. This would then be reflected in a coupling constant  $\gamma_\delta$ , sufficiently large to suppress  $\delta$  below  $T_c$  but sufficiently small to avoid a first order transition between both states. The temperature variation of  $\delta$  is, however, very reminiscent of the behavior of the ordered magnetic moment, which has been shown to be strongly suppressed below  $T_c$  in Refs. [14,15]. Understanding both phenomena would require the simultaneous fine-tuning of the phase competitions, i.e., of  $\gamma_\delta$  and the corresponding coupling constant  $\gamma_m$ , describing the interaction between magnetism and superconductivity via  $\frac{\gamma_m}{2} (\mathbf{m}_1^2 + \mathbf{m}_2^2) |\Psi|^2$ , where  $\mathbf{m}_1$  and  $\mathbf{m}_2$  are the staggered magnetizations corresponding to the two Fe sites in the basal plane.

An intriguing alternative explanation of our results is rooted in the unusual magnetoelastic coupling of the iron arsenides and the competition between superconductivity and magnetism. First, we again note that commensurate antiferromagnetic fluctuations, of the kind seen in the iron arsenides, have been shown to lead to an emergent, nematic

order parameter [16],  $\varphi = \mathbf{m}_1 \cdot \mathbf{m}_2$ . As discussed in detail in Refs. [19–21],  $\mathbf{m}_1$  and  $\mathbf{m}_2$  are weakly coupled and their relative orientation is only fixed once nematic order sets in so that  $\langle \varphi \rangle \neq 0$ . Nematic ordering occurs when the correlation length for spin fluctuations,  $\xi$ , reaches a finite threshold value [21]. We emphasize here that nematic ordering transpires via the spin fluctuations of the system and does not require static magnetic ordering. Therefore, nematic order, and the associated structural distortion, discussed below, can occur above the magnetic transition, or even in its absence. This is consistent with the fact that the tetragonal-to-orthorhombic transition occurs at temperatures above the onset of static magnetic order (see Fig. 4) and our observation of a tetragonal-to-orthorhombic transition for the  $x = 0.063$  sample in the absence of static magnetic order down to 2 K [24].

To understand the coupling between nematic order and the lattice distortion we consider the leading terms in  $\delta$  that contribute to the free energy,  $\lambda\delta\varphi + \frac{C_{s,0}}{2}\delta^2$ , with the bare shear modulus,  $C_{s,0}$ , and coupling constant,  $\lambda$ . Minimizing the free energy with respect to  $\delta$  leads to the relation  $\delta = -\frac{\lambda}{C_{s,0}}\langle \varphi \rangle$ ; the lattice distortion simply follows the nematic order parameter. Simultaneous orthorhombic and nematic ordering lifts the magnetic frustration and allows magnetic long-range order.

Both the suppression of magnetic long-range order below  $T_c$  [14,15] and the suppression of the orthorhombicity described here can be understood as a consequence of the competition between itinerant magnetism and superconductivity for the same electrons. In the superconducting state, the magnetic fluctuations are modified. We have already noted, for example, the opening of a gap and the appearance of a resonance in several inelastic neutron scattering measurements [9–15], illustrating a change in the spin dynamics in the superconducting phase. This competition between magnetism and superconductivity also leads to a decrease in the spin fluctuation correlation length,  $\xi$  [21]. From the discussion above, it then follows that superconductivity weakens the magnetic spin fluctuations below  $T_c$ , hence, suppressing the nematic order and the consequent orthorhombic distortion.

In summary, our high-resolution x-ray diffraction measurements have revealed an unusually strong response of the lattice to superconductivity in  $\text{Ba}(\text{Fe}_{1-x}\text{Co}_x)_2\text{As}_2$ , leading to a tetragonal structure for  $x \approx 0.063$ . We propose that the coupling between the orthorhombic distortion and superconductivity is indirect and arises from the strong competition between magnetism and superconductivity, together with a strong magnetoelastic coupling in the form of emergent nematic order. The appeal of this scenario is that no new direct coupling between the elastic and superconducting order parameters is required.

We thank A. Kracher for the WDS measurements. The work at the Ames Laboratory was supported by the U.S.

DOE, office of science, under Contract No. DE-AC02-07CH11358.

\*goldman@ameslab.gov

- [1] Y. Kamihara, T. Watanabe, M. Hirano, and H. Hosono, *J. Am. Chem. Soc.* **130**, 3296 (2008).
- [2] M. Rotter, M. Tegel, and D. Johrendt, *Phys. Rev. Lett.* **101**, 107006 (2008).
- [3] Q. Huang, Y. Qiu, W. Bao, M. A. Green, J. W. Lynn, Y. C. Gasparovic, T. Wu, G. Wu, and X. H. Chen, *Phys. Rev. Lett.* **101**, 257003 (2008).
- [4] A. Jesche *et al.*, *Phys. Rev. B* **78**, 180504(R) (2008).
- [5] A. I. Goldman, D. N. Argyriou, B. Ouladdiaf, T. Chatterji, A. Kreyssig, S. Nandi, N. Ni, S. L. Bud'ko, P. C. Canfield, and R. J. McQueeney, *Phys. Rev. B* **78**, 100506(R) (2008).
- [6] S. E. Hahn *et al.*, *Phys. Rev. B* **79**, 220511(R) (2009).
- [7] R. Mittal *et al.*, *Phys. Rev. B* **79**, 144516 (2009).
- [8] L. Chauvière, Y. Gallais, M. Cazayous, A. Sacuto, M. A. Méasson, D. Colson, and A. Forget, *Phys. Rev. B* **80**, 094504 (2009).
- [9] A. D. Christianson *et al.*, *Nature (London)* **456**, 930 (2008).
- [10] S. Chi *et al.*, *Phys. Rev. Lett.* **102**, 107006 (2009).
- [11] M. D. Lumsden *et al.*, *Phys. Rev. Lett.* **102**, 107005 (2009).
- [12] S. Li, Y. Chen, S. Chang, J. W. Lynn, L. Li, Y. Luo, G. Cao, Z. Xu, and P. Dai, *Phys. Rev. B* **79**, 174527 (2009).
- [13] D. S. Inosov, J. T. Park, P. Bourges, D. L. Sun, Y. Sidis, A. Schneidewind, K. Hradil, D. Haug, C. T. Lin, B. Keimer, and V. Hinkov, *Nature Phys.*, doi:10.1038/nphys1483 (2009).
- [14] D. K. Pratt, W. Tian, A. Kreyssig, J. L. Zarestky, S. Nandi, N. Ni, S. L. Bud'ko, P. C. Canfield, A. I. Goldman, and R. J. McQueeney, *Phys. Rev. Lett.* **103**, 087001 (2009).
- [15] A. D. Christianson, M. D. Lumsden, S. E. Nagler, G. J. MacDougall, M. A. McGuire, A. S. Sefat, R. Jin, B. C. Sales, and D. Mandrus, *Phys. Rev. Lett.* **103**, 087002 (2009).
- [16] P. Chandra, P. Coleman, and A. I. Larkin, *Phys. Rev. Lett.* **64**, 88 (1990).
- [17] T. Yildirim, *Phys. Rev. Lett.* **101**, 057010 (2008).
- [18] Q. Si and E. Abrahams, *Phys. Rev. Lett.* **101**, 076401 (2008).
- [19] C. Fang, H. Yao, W.-F. Tsai, J. Hu, and S. A. Kivelson, *Phys. Rev. B* **77**, 224509 (2008).
- [20] C. Xu, M. Müller, and S. Sachdev, *Phys. Rev. B* **78**, 020501(R) (2008).
- [21] R. M. Fernandes, L. H. VanBebber, S. Bhattacharaya, P. Chandra, V. Keppens, D. Mandrus, M. A. McGuire, B. C. Sales, A. S. Sefat, and J. Schmalian, arXiv:0911.3084 (unpublished).
- [22] N. Ni, M. E. Tillman, J.-Q. Yan, A. Kracher, S. T. Hannahs, S. L. Bud'ko, and P. C. Canfield, *Phys. Rev. B* **78**, 214515 (2008).
- [23] C. Meingast, O. Krauf, T. Wolf, H. Wühl, A. Erb, and G. Müller-Vogt, *Phys. Rev. Lett.* **67**, 1634 (1991).
- [24] R. M. Fernandes *et al.*, arXiv:0911.5183 (unpublished).